ACS OMEGA

Open Access

http://pubs.acs.org/journal/acsodf

Article

Sorption Studies of Eu^{3+} Ions Using YPO_4 and YPO_4:20% Ce Nanoparticles, Optical Properties, and in Conjunction with Instrumental Neutron Activation Analysis

Ramaswamy Sandeep Perala, Venkata Nagendra Kumar Putta,* Bheeshma Pratap Singh, Raghumani Singh Ningthoujam,* and Raghunath Acharya*

Cite This: *ACS Omega* 2025, 10, 14616−14625

Read Online

ACCESS | Metrics & More | Article Recommendations | Supporting Information

ABSTRACT: The contamination of rare earth (RE) ions in an aqueous medium causes severe health hazards due to their toxicity. Hence, the removal of RE ions is necessary. In this work, we have used a concept of host−guest interaction which assists in the removal of RE ions by choosing the host as YPO_4 nanomaterial and the Eu^{3+} as foreign/guest ions. The YPO_4 host having two different phases like tetragonal (pure YPO_4) as well as hexagonal structure (20 at. % Ce^{3+}-doped YPO_4) are used for comparative studies. A sorption study of Eu^{3+} was carried out with varying amounts of host (YPO_4 and/or YPO_4:20% Ce) at different pH values, i.e., 3 (acidic), 7 (neutral), and 12 (basic). The loading capacity of the host was studied via instrumental neutron activation analysis (INAA) and photoluminescence (PL) experiments. Here, the role of quenching is clearly explained in the PL. INAA is very sensitive to europium owing to its higher absorption cross-section ($\sigma \sim 9.2 \times 10^3$ barn) and lower half-life (9.3 h). INAA using a short irradiation facility at PCF of the Dhruva reactor (1 min flux of neutrons at 5×10^{13} n/cm^2/s) was effectively used to study the uptake of Eu^{3+} using its activation product ^{152m}Eu (multi-γ-rays like 122, 344, and 842 keV). The order of uptake of Eu^{3+} ions over nanoparticles is acidic < neutral < basic medium. In the acidic medium (pH = 3), emission peaks at ∼590 and ∼615 nm could not be observed due to low sorption of Eu^{3+} over the host, whereas in the alkaline medium (pH = 12), their emission peaks are observed. It is interesting that at neutral pH, its uptake capacity is very good, and this has got a real case sample application for the removal of lanthanides.

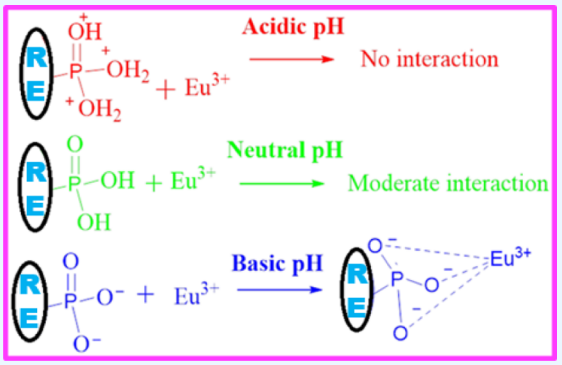

1. INTRODUCTION

In recent years, synthesis of rare earth ion (Ln^{3+})-doped nanomaterials has attracted massive interest due to their vast applications.[1−7] Nanomaterials exhibit different chemical and physical properties and have a high surface area as compared to bulk.[8,9] In this perspective, there are many potential host materials like $LaPO_4$, YVO_4, $GdVO_4$, Y_2O_3, YPO_4, Gd_2O_3, $GdPO_4$, etc.[10−16] Among these host materials, YPO_4 is an interesting and excellent host material.[17,18] For many lanthanide activators, YPO_4 is used as a host material.[16,19] To remove ions from different environmental matrices, it is essential to design methods and a number of methods have been designed for this purpose.[20,21]

For the removal of ionic wastes, ion exchange is an effective process.[22−25] Among the different activators like natural inorganic cation interactions or exchanges, for instance, zeolites and clays are widely used for the elimination of radioactive ions from aqueous media. However, this type of procedure takes maximum time, so its real application in a real system is indefinite. Another alternative procedure that is extensively utilized is precipitation to separate the target ions from aqueous media. It is an advantageous procedure due to its characteristics of simple, fast, and low operational cost. But it needs a high-concentration precipitate of at least one component. Hence, this type of procedure could not be used in the case of trace concentration levels. Various solid materials are being explored at present for ecological decontamination.[26−30] Nevertheless, there are limitations such as nonselectivity, difficulty of separation from a medium, low sorption capability, etc., and consequently, there is a lot of research taking place in finding an appropriate extractant that can meet all the chosen criteria of a perfect sorbent. Therefore, this type of combined or adsorbed nanoparticles are mainly utilized for the elimination of toxic materials from the environmental system.[14,15,31]

Received: July 24, 2024
Revised: December 13, 2024
Accepted: December 16, 2024
Published: April 8, 2025

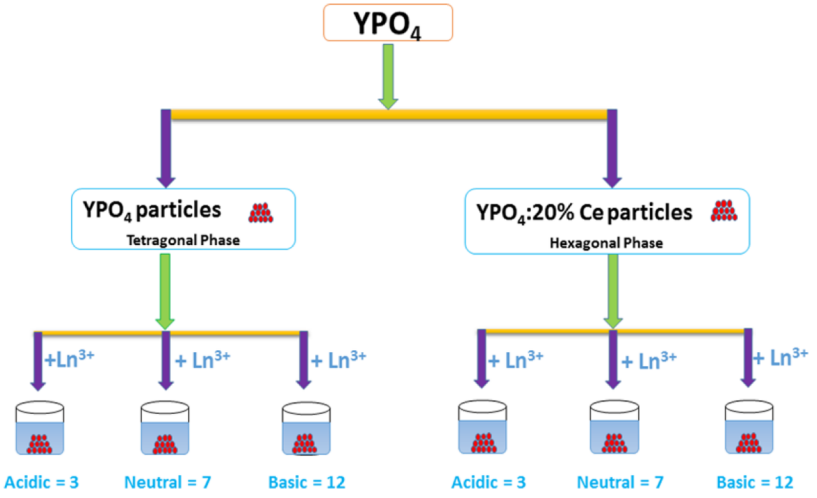

Figure 1. Schematic diagram illustrating the sorption of Ln^{3+} ions on nanoparticles at different pH values.

In our present investigation, we explore YPO_4 (tetragonal phase)- and YPO_4:20% Ce (hexagonal phase)-doped nanoparticles that are used as a host solid material/matrix (inactive) for the removal of Eu^{3+} ions (i.e., guest particles, active in luminescence) from aqueous media as a model. Here, Eu^{3+} ions in different ppm levels (i.e., 80, 60, and 40 ppm) are prepared. It is important to identify the effect of Eu^{3+} ions on sorption. Different parts per million levels of Eu^{3+} ions were selected, and their uptake on nanoparticles from aqueous media was studied. To date, there has been no discussion to the best of the authors' knowledge.

The experiments were performed at three different pH values ~3, ~7, and ~12 by adjusting the pH using NH_4OH and HCl to examine the effective uptake of Eu^{3+} ions, their settlement on nanoparticle was discussed, and its schematic for better understanding is shown in Figure 1. To the best of the authors' knowledge, this is the first report on the separation of Eu^{3+} ions at different ppm levels and pH levels, and their uptake/sorption results were interconnected with the standard/parent solution of Eu^{3+} ions evaluated via the INAA (instrumental neutron activation analysis) technique, whose uptake is examined by using PL characterization and the luminescence properties are studied extensively.

2. RESULTS AND DISCUSSION

2.1. XRD Study. Figure 2a,b displays the XRD patterns of the as-prepared tetragonal (YPO_4) and hexagonal (YPO_4 doped with 20% Ce) samples. The as-prepared YPO_4 nanoparticles have a tetragonal phase (i.e., xenotime mineral type tetragonal structure), whereas YPO_4 doped with 20% Ce nanoparticles have a hexagonal phase and compared with standard JCPDF card no. 11−0254 (red color asterisks in Figure 2a for the tetragonal phase) and JCPDF card no. 42−0082 (red color asterisks in Figure 2b for the hexagonal phase) structures, with their concerned *hkl* planes, respectively. It is revealed that there are no extra peaks evolved or formed during the synthesis process, which is confirmed by XRD study. Ethylene glycol (EG) was used as a solvent for the preparation of nanoparticles as it can act as a reaction medium as well as a capping agent, thus governing the limiting of particle growth.[32,33] Therefore , it clearly shows the formation of a tetragonal phase in the case of YPO_4 and a hexagonal phase in the case of YPO_4:20% Ce-doped nanoparticles. The transition

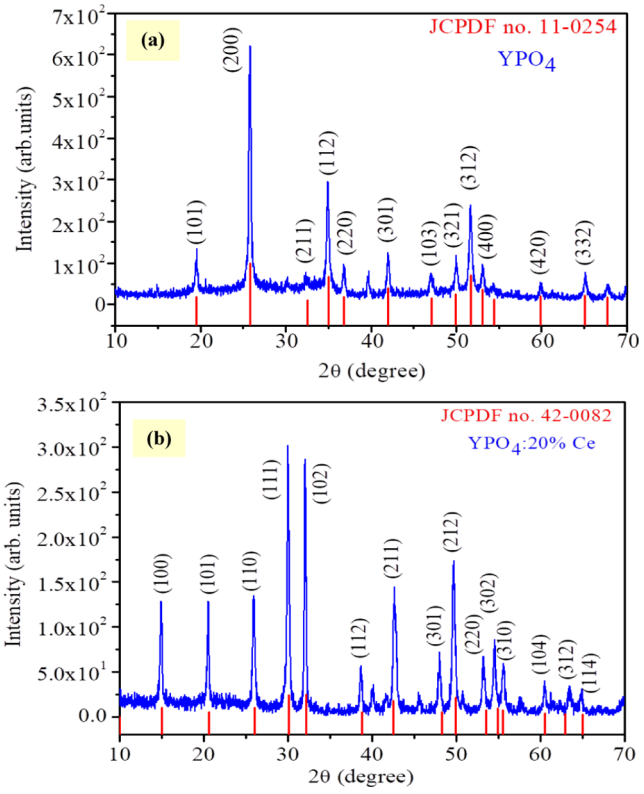

Figure 2. Typical XRD patterns of (a) YPO_4 (tetragonal phase) nanoparticle with JCPDF no. 11−0254 (indicated by red color asterisks lines) and (b) YPO_4:20% Ce (hexagonal phase) nanoparticle with JCPDF no. 42−0082 (indicated by red color asterisks lines).

from a mixture of tetragonal and hexagonal phases to a purely hexagonal phase is attributed to the incorporation of larger ionic Eu^{3+} and Ce^{3+} ions into the lattice structure.[1,17] The hexagonal phase remains stable exclusively when larger ionic-sized ions replace the Y^{3+} sites. The ionic radii for Y^{3+}, Ce^{3+}, and Eu^{3+} with the coordination number of 8 are 1.019, 1.143, and 1.066 Å, respectively.[34] A few extra peaks are observed due to the association of the mixture of both phases.

So, the lattice parameters ($a = b$, c) and the volume of two different phase structures are calculated by using UnitCellWin software. The lattice parameters estimated are a = 6.937 Å, c =

https://doi.org/10.1021/acsomega.4c06813
ACS Omega 2025, 10, 14616−14625

5.942 Å, and unit cell volume V = 285.998 Å^3 for the tetragonal phase structure, and a = 6.837 Å, c = 6.297 Å, and unit cell volume V = 254.931 Å^3 for the hexagonal phase structure.

For selecting the as-prepared YPO_4 and YPO_4:20% Ce as a host material, their chemical stability at different pH levels, i.e., at pH = 3 (acidic), 7 (neutral), and 12 (basic), and XRD patterns are shown in Figure S1a,b. Thus, the peak positions of XRD patterns are almost unchanged, confirming the stability of the host nanoparticles.

Bragg's relation explains the interplanar distance (d_{hkl}) of plane (hkl) in a lattice and is given by

$$2d_{hkl}\sin\theta = n\lambda \quad (1)$$

where hkl represents the plane, λ represents the wavelength of Cu−K_α radiation, and θ represents Bragg's angle.

The average crystallite size (D) has been calculated by using the Debye−Scherrer equation:

$$D = \frac{0.89\lambda}{\beta\cos\theta} \quad (2)$$

where λ represents the wavelength, β represents the full width at half-maximum (FWHM) of the hkl plane, and θ represents the angle of diffraction. The average crystallite sizes for YPO_4 and 20% Ce-doped YPO_4 are calculated to be ∼60 and ∼70 nm, respectively.

2.2. SEM and TEM Studies. Figure 3 shows a scanning electron microscopy (SEM) image of YPO_4. The prepared

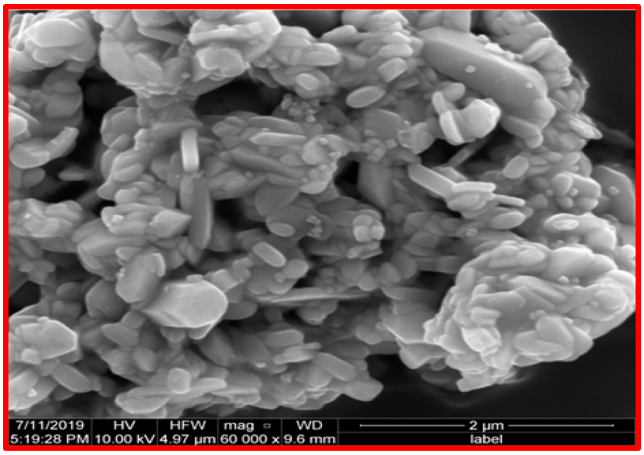

Figure 3. SEM micrograph of the YPO_4 (tetragonal phase) nanoparticle.

nanophosphor is annealed at 900 °C for 4 h in a furnace. The micrograph shows a large number of rectangular and spherical shapes accompanied by a small portion of cuboidal shapes. Here, the average size found from the rectangular-shaped particles is ∼70 nm.

From Figure 4 (TEM image of YPO_4 nanoparticles), it is evident that the micrograph exhibits an agglomerated particle with an approximate size of ∼70 nm. For the preparation of TEM Cu grid, the nanoparticles (2 mg) are dispersed in methanol (5 mL) and sonicated for 5 min. One drop was added over Cu grid for the investigation of the size of the nanoparticles.

2.3. FTIR Study. Figure 5 shows the FTIR spectrum of the YPO_4 nanoparticles. The strong bands observed at ∼1630 and ∼3430 cm^{-1} correspond to bending and stretching vibrations of water (H_2O) particles present on the surface.[3] The typical

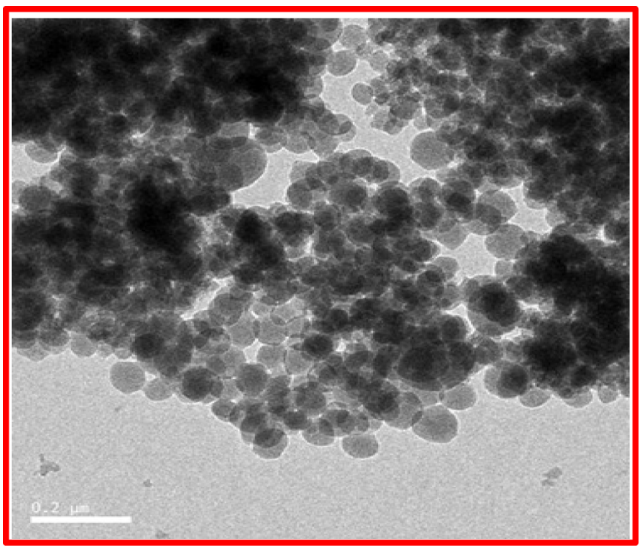

Figure 4. TEM micrograph of the YPO_4 (tetragonal phase) nanoparticle.

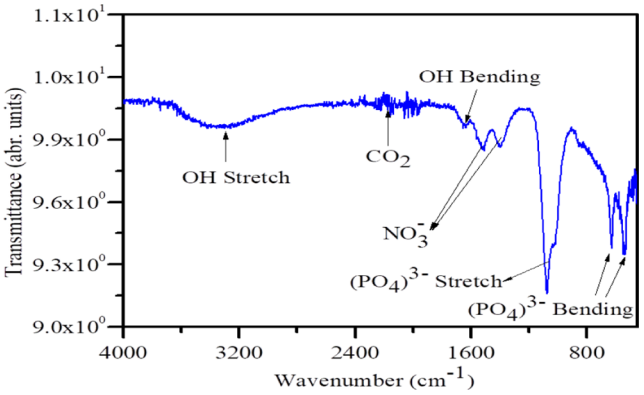

Figure 5. Fourier transform infrared (FT-IR) spectrum of the YPO_4 nanoparticles.

peaks of bending vibrations of $(PO_4)^{3-}$ (ν_4 vibrations) are observed at ∼530 and 651 cm^{-1}, whereas the strong merged bands of stretching vibration of $(PO_4)^{3-}$ (ν_3 vibrations) are observed at ∼1005 and ∼1093 cm^{-1}. A strong peak observed at ∼1630 and ∼1650 cm^{-1} signifies the presence of NO_3^-. Similar bands are also observed in the YPO_4:20% Ce nanophosphor.

2.4. Sorption of Eu^{3+} Ion Loading over YPO_4 and YPO_4:20%Ce Nanoparticle Surface at Different pH Levels (pH = 3, 7, and 12). *2.4.1. Tetragonal Phase at pH = 3, 7, and 12.* For the tetragonal YPO_4 nanomaterial, 50 mg was weighed and transferred into a host bottle, which is assumed as a host matrix, and 10 mL of 80 ppm Eu^{3+} solution was transferred into the bottle, which is considered as control or parent stock. Another bottle containing 50 mg of host material and 10 mL of Eu^{3+} solution was maintained in an acidic condition by adding dil. HCL; and its pH was maintained at pH = 3 by checking with pH paper. Similarly, 10 mL of 80 ppm Eu^{3+} solution was added to the 50 mg host bottle and maintained under neutral conditions at pH = 7. Another 10 mL of 80 ppm Eu^{3+} solution was added to the 50 mg host bottle, and it is maintained under basic conditions at pH = 12. The same experiment was triplicated for the above pH conditions, and each bottle was properly packed with

https://doi.org/10.1021/acsomega.4c06813
ACS Omega 2025, 10, 14616−14625

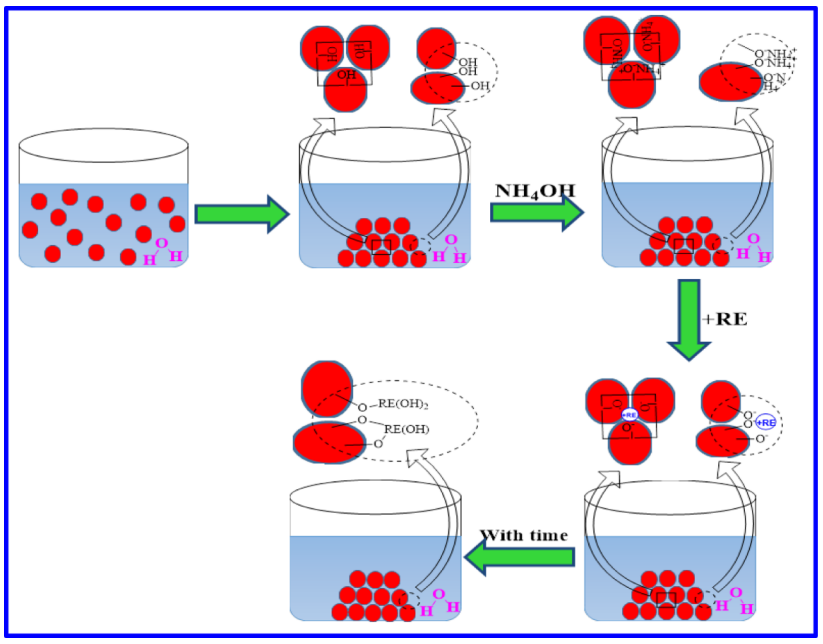

Figure 6. Schematic illustration of the uptake of Eu^{3+} ions on host matrices (YPO_4 and YPO_4:20% Ce) nanoparticles.

Teflon for 1 day before being ultrasonicated for 10 min. The next day, they were transferred into a centrifuge tube and centrifuged at 5000 rpm for 10 min in which the supernatant was transferred into the host bottle for further studies such as NAA and the residue was for PL study. The residue was washed with 5 mL of acetone thrice. These centrifuge tubes were properly numbered according to their host bottles and dried under an IR lamp to collect the dry powder samples. The dry powder residue was used for characterizations like XRD, FT-IR, luminescence, etc.

Similar experiments were performed by changing the weight of the host matrix (for 100 and 200 mg) and changing the Eu^{3+} concentrations down to 60 and 40 ppm, respectively. The mechanism involved in the interaction of the host and guest matrix is well explained via the schematic diagram in Figure 6 for better understanding.

2.4.2. Hexagonal Phase at pH = 3, 7, and 12. The above experimental process is the same in the case of the YPO_4:20% Ce (hexagonal) phase as well. So, in both cases, the collected residue and supernatant were further examined to determine the uptake of Eu^{3+} ions on the host matrices and also to determine the remaining concentration present in the supernatant.

2.5. Photoluminescence Study. *2.5.1. Excitation Study.* Figure 7 shows the excitation spectrum of Eu^{3+} ions, which is adsorbed on solid matrix YPO_4 (50 mg) monitored at ~615 nm emission (residue obtained at pH = 12). A broad emission range is observed from 240 to 390 nm with a maximum peak at 320 nm. A prominent excitation peak is observed in the spectrum at approximately 265 nm, which is associated with the Eu−O charge transfer band (CTB). This phenomenon primarily results from the transition of 2p electrons from the O^{2-} orbitals to the vacant 4f orbitals of Eu^{3+} ions. Additionally, absorption peaks for Eu^{3+} are detected at around 320, 380, and 395 nm, which correspond to the transitions like $^7F_{0,1} \rightarrow {}^5H_{3,6}$, $^7F_{0,1} \rightarrow {}^5G_1$, $^5L_6$, and $^7F_{0,1} \rightarrow {}^5L_6$, respectively.[35]

2.5.2. Emission Study. If the emitted radiative light (E_{em}) is lower than the excited light (E_{exc}), i.e., if $E_{em} < E_{exc}$, then this

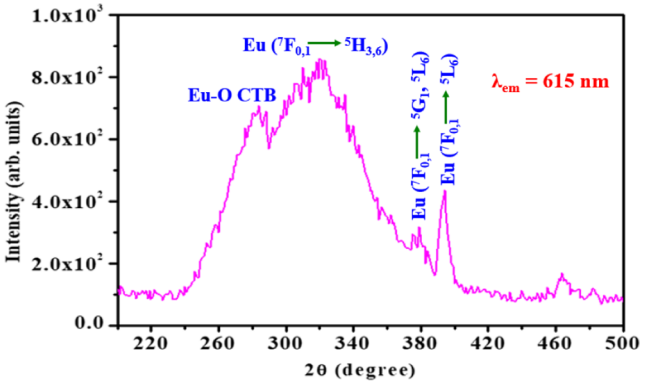

Figure 7. Excitation spectrum of Eu^{3+} ions absorbed on YPO_4 (50 mg experiment performed at pH = 12) at excitation of λ_{em} = 615 nm.

type of process is called Stokes shift or down conversion process. Upon UV excitation at 395 nm (direct excitation), the emission spectrum of Eu^{3+} was loaded on YPO_4 nanoparticles. Different levels of 80, 60, and 40 ppm Eu^{3+} ions loaded on YPO_4 and YPO_4:20% Ce were studied for luminescence and the emission peaks of activator ions were observed at ~595 nm, ~615 nm, ~655 nm, and ~695 nm emission bands which are related to $^5D_0 \rightarrow {}^7F_1$, $^5D_0 \rightarrow {}^7F_2$, $^5D_0 \rightarrow {}^7F_3$, and $^5D_0 \rightarrow {}^7F_4$ electronic transitions of an Eu^{3+} ion, respectively.[35] The emission spectra of different parts per million levels were monitored at an excitation wavelength of 395 nm. Every excitation displays the emission peaks due to Eu^{3+} ion.

For the case of 80 ppm uptake of Eu^{3+} on YPO_4 (50 mg) and YPO_4:20%Ce (50 mg) nanoparticles, their luminescence spectra under 395 nm excitation at different pH are shown in Figure 8a,b. Interestingly, a difference in emission intensity was observed. The difference in the uptake of Eu^{3+} (guest) ions was mainly influenced by the microstructure of the host material. Hitherto, the experiment reveals that the uptake is maximum in the hexagonal phase of YPO_4 rather than the tetragonal phase of YPO_4.[36] Emission intensity is poor in the case of YPO_4:20% Ce nanoparticles. This is due to the presence of water in the

https://doi.org/10.1021/acsomega.4c06813
ACS Omega 2025, 10, 14616−14625

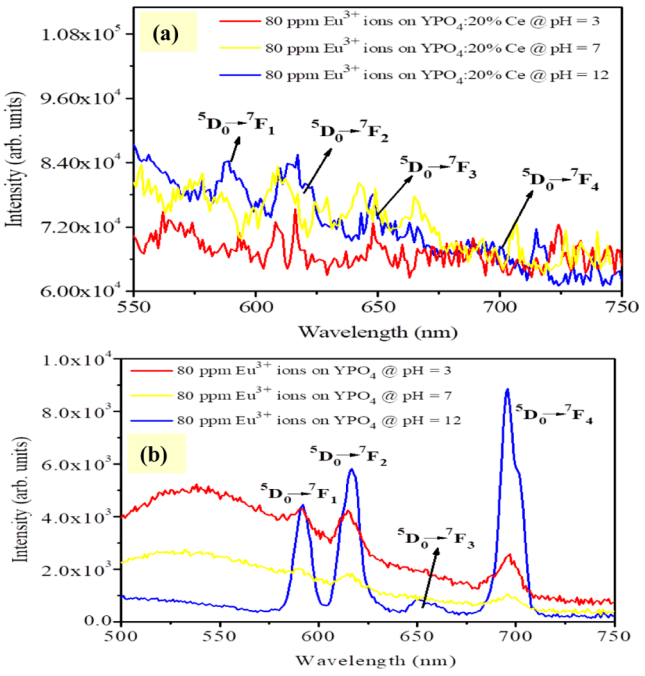

Figure 8. Emission spectra of residue (50 mg) separated after 80 ppm Eu^{3+} ions loaded at different pH = 3, 7, and 12 values and excited at λ_{exc} = 395 nm of (a) YPO_4:20% Ce (hexagonal phase) nanoparticles and (b) YPO_4 (tetragonal phase) nanoparticles along with their energy levels.

pores of the hexagonal lattice.[36] In the case of the tetragonal phase (YPO_4), luminescence intensity is good. However, Eu^{3+} ions absorbed on nanoparticles at pH = 12 show strong luminescence intensity compared to that at pH = 3 or 7.

In the case of 60 ppm uptake of Eu^{3+} on YPO_4 (50 mg) and YPO_4:20%Ce (50 mg) nanoparticles, the luminescence intensity for YPO_4 (tetragonal phase) is stronger than that of YPO_4:20%Ce (hexagonal phase), as shown in Figure 9a,b. For YPO_4 (tetragonal phase), the luminescence intensity at pH = 12 is much stronger than that at pH = 7, followed by that at pH = 3.

In the case of 40 ppm uptake of Eu^{3+} on YPO_4 (50 mg) and YPO_4:20%Ce (50 mg) nanoparticles, the luminescence intensity for YPO_4 (tetragonal phase) is stronger than that of YPO_4:20%Ce (hexagonal phase), as shown in Figure 10ab. For YPO_4 (tetragonal phase), the luminescence intensity at pH = 12 is much stronger than that at pH = 7, followed by that at pH = 3.

Upon comparison of the emission spectra of 40, 60, and 80 ppm uptake of Eu^{3+} on YPO_4 (50 mg), the luminescence intensity of Eu^{3+} ions decreases from 80 ppm uptake to 40 ppm uptake on nanoparticles. This suggests that the uptake of Eu^{3+} ions is related to the amount of Eu^{3+} ions present in the solution. After confirmation of the uptake of Eu^{3+} ions on the host matrix by luminescence, the amount of uptake is also determined by using the NAA technique. Here, the supernatant which is separated from the residue is utilized for examining the uptake. The above luminescence clearly shows that due to quenching in the hexagonal phase, we could not be able to see the luminescence, and in the case of the tetragonal phase, we could observe the luminescence of europium in three different mediums. In this experiment, the rare-earth phosphates (YPO_4 and YPO_4:20% Ce) are used as a host and absorbed Eu^{3+} ions act as an luminescence activator.[37,38] As the

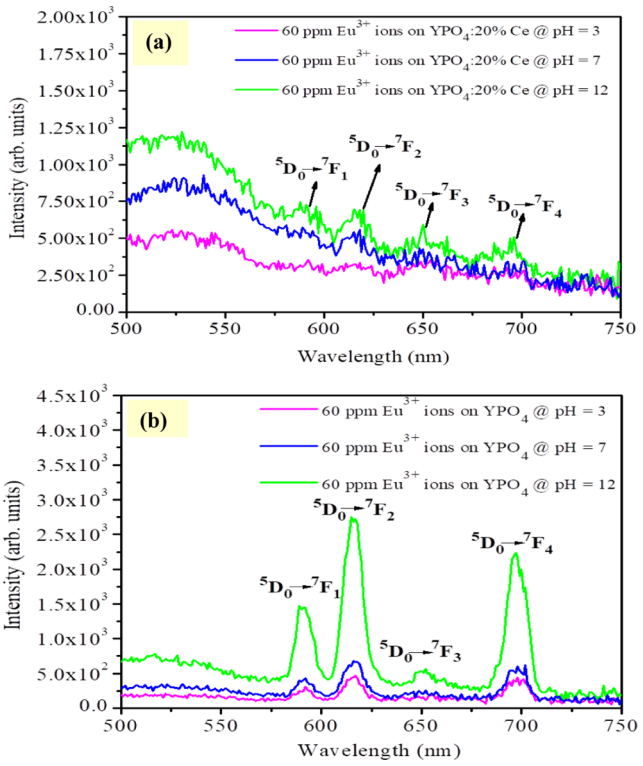

Figure 9. Emission spectra of residue (50 mg) separated after 60 ppm Eu^{3+} ions loaded at different pH = 3, 7, and 12 values and excited at λ_{exc} = 395 nm of (a) YPO_4:20% Ce (hexagonal phase) nanoparticles and (b) YPO_4 (tetragonal phase) nanoparticles along with their energy levels.

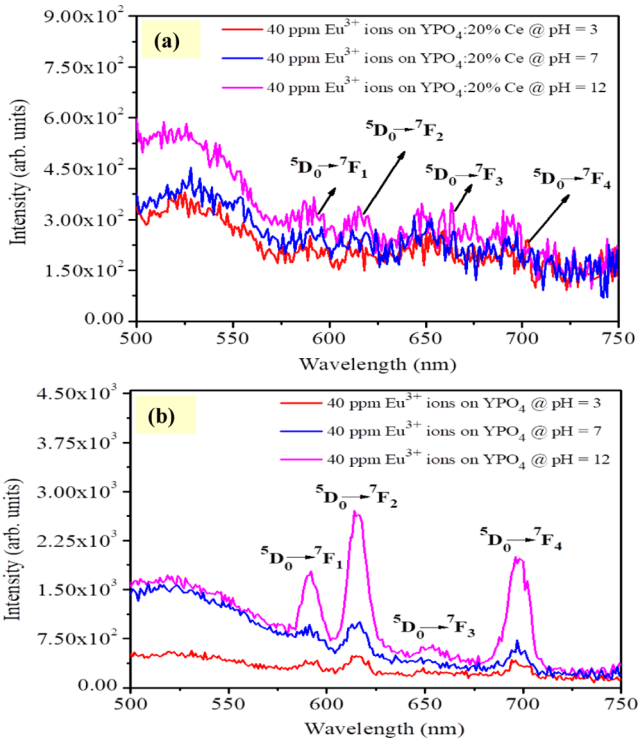

Figure 10. Emission spectra of residue (50 mg) separated after 40 ppm Eu^{3+} ions loaded at different pH = 3, 7, and 12 values and excited at λ_{exc} = 395 nm of (a) YPO_4:20% Ce (hexagonal phase) nanoparticles and (b) YPO_4 (tetragonal phase) nanoparticles along with their energy levels.

https://doi.org/10.1021/acsomega.4c06813
ACS Omega 2025, 10, 14616−14625

ionic size of the doping RE^{3+} increases, there will be a distortion in the crystal structure of the $REPO_4$ from tetragonal to monoclinic.[39] Interestingly, if the water molecules (2−3) are grouped in the unit cell during the preparation, a hexagonal phase is formed regardless of the ionic size of the RE^{3+}, even at higher temperatures (say up to 500 °C). Zollfrank et al.[40] have reported that the water molecules in the $EuPO_4$ are even stable at a higher temperature, ∼600 °C. A similar observation by Luwang et al.[17] well explained that the stability of water in hexagonal pores remained up to 800 °C in Ce^{3+}-doped YPO_4:Eu^{3+} nanoparticles. Due to this trapping of the water molecules in the pores of the hexagonal phase of YPO_4, the luminescence intensities are completely absent in the PL experiment due to the quenching effect.[17] So, from Figures 8a, 9a, and 10a, the luminescence intensity of Eu^{3+} is completely quenched in the hexagonal phase of YPO_4.

2.6. Analysis of Eu^{3+} Ions by the NAA Technique. *2.6.1. Sample Preparation.* The supernatant, which is collected after the separation of adsorption studies, was examined to determine the remaining percentage of guest (Eu^{3+}) material present in the supernatant liquid by using the INAA (instrumental neutron activation analysis) technique. By using a pipette, the supernatant liquid was measured to 50 μL and dried on a Whatman filter paper. The dried paper was packed completely in a pouch, and the various pouches were sealed in a capsule for irradiation in the Dhruva Reactor, BARC.

2.6.2. Analysis by the NAA Technique. The loading capacity of the host was studied via instrumental neutron activation analysis (INAA) and photoluminescence experiments. INAA is very sensitive to europium owing to its higher absorption cross-section ($\sigma \sim 9.2 \times 10^3$ barn) and lower half-life (9.3 h). INAA using the short irradiation facility at the PCF of the Dhruva reactor (1 min flux of neutrons at 5×10^{13} n/cm^2/s) was effectively used to study the uptake of Eu^{3+} using its activation product ^{152m}Eu (multi-γ-rays like 122, 344, and 842 keV). The order of uptake of Eu^{3+} ions over nanoparticles is acidic < neutral < basic medium. The typical INAA spectrum of the europium ion can be seen in Figure 11.

In the case of 80 ppm uptake of Eu^{3+} on YPO_4 and YPO_4:20%Ce nanoparticles (50, 100, and 200 mg) at pH = 3 (acidic), 7 (neutral), and 12 (alkaline), analysis after INAA results are shown in Figure 12a,b. The percentage absorption of Eu^{3+} ions on nanoparticles increases with the increase of host amount from 50 mg to 100 mg and then to 200 mg of both nanoparticles. Also, the percentage absorption of Eu^{3+} ions on nanoparticles increases with an increase of the pH of the medium from acidic to neutral to alkaline.

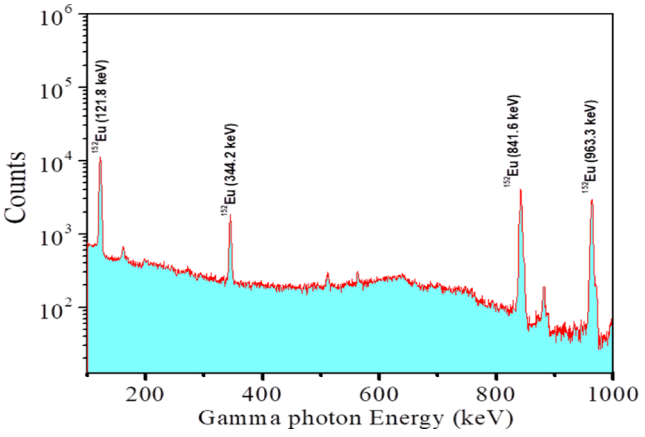

Figure 11. Typical INAA spectrum of Eu^{3+} remaining in the supernatant.

In the case of 60 ppm uptake of Eu^{3+} on YPO_4 and YPO_4:20%Ce nanoparticles (50, 100, and 200 mg) at pH = 3 (acidic), 7 (neutral), and 12 (alkaline), analysis after INAA results is shown in Figure 13a,b. The trend of Eu^{3+} ion uptake is similar to that of 80 ppm uptake.

In the case of 40 ppm uptake of Eu^{3+} on YPO_4 and YPO_4:20%Ce nanoparticles (50, 100, and 200 mg) at pH = 3 (acidic), 7 (neutral), and 12 (alkaline), analysis after INAA results is shown in Figure 14a,b. A slight variation in the percentage of Eu^{3+} ion uptake by nanoparticles is observed as compared to those of 80 and 60 ppm uptake.

So, the uptake has been thoroughly studied by using the NAA technique, and most of the guest (Eu^{3+}) ion is being adsorbed on to the host matrix. Further a general possible mechanism is proposed for better understanding. In the case of tetragonal phase, a PL study can prove the sorption capacity of Eu^{3+} ions, where the hexagonal phase could not identify the sorption capacity of Eu^{3+} ions as its luminescence intensity is very weak. Using the INNA technique, it is confirmed that the sorption capacity of the hexagonal phase is more than that of the tetragonal phase toward Eu^{3+} ions.

2.6.3. Effect of Different pH of the Coagulation of Eu^{3+} Ions on the Nanoparticle. The general hypothesis involved in the uptake of guest ion onto the host matrix is schematically given in Figure 15. It is assumed that, in the case of acidic (pH = 3), there may be very less interaction due to the positive nature of protons and europium ions which get repulsion. Consequently, in the case of neutral (pH = 7), there may be a moderate interaction by the formation of few europium ions into europium hydroxide ions. However, in the case of basic (pH = 12), there is a chance of the formation of europium hydroxide with the OH^- group. So, the uptake of europium ion on a host matrix is more when compared to different pH values.

3. CONCLUSIONS

Tetragonal and hexagonal yttrium phosphate nanoparticles are synthesized successfully. The selected uptakes of Eu^{3+} ions on host materials *h*-$YPO_4.xH_2O$ and *t*-YPO_4 have been observed. So, a complete investigation is carried out to understand the most uptake in the case of 50, 100, and 200 mg of the tetragonal and hexagonal phases via three different pH levels. Both phases such as tetragonal and hexagonal structures are stable in acidic, neutral, and alkaline mediums. The uptake of europium ions is confirmed by photoluminescence. The uptake study of the tetragonal phase of YPO_4 nanoparticles as well as the hexagonal phase of YPO_4:20% Ce nanoparticles has weak luminescence in acidic medium. For the first time, the uptake is extensively studied by utilizing INAA, using a short irradiation facility at the PCF of the Dhruva reactor (1 min flux of neutrons at 5×10^{13} n/cm^2/s), and the study regarding the uptake of Eu^{3+} ions is monitored from activation product ^{152m}Eu (multi-γ-rays like 122, 344, and 842 keV). Individually, the tetragonal phase of YPO_4 nanoparticles and the hexagonal phase of YPO_4:20% Ce nanoparticles have shown the percentage uptake of Eu^{3+} ions using INAA techniques. In the case of tetragonal phase, the PL study can prove the sorption capacity of Eu^{3+} ions, whereas in the hexagonal phase, it could not identify the sorption capacity of Eu^{3+} ions as its

https://doi.org/10.1021/acsomega.4c06813
ACS Omega 2025, 10, 14616−14625

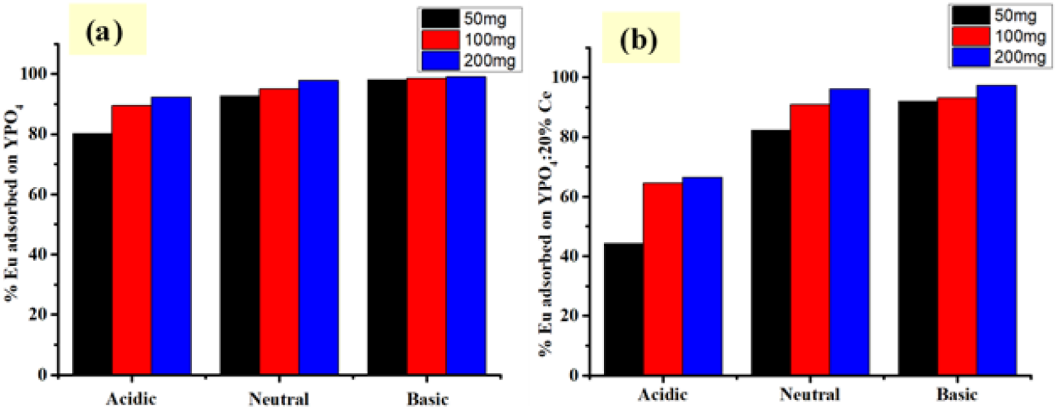

Figure 12. NAA data of supernatant separated after 80 ppm Eu^{3+} ions loaded on different amounts (X = 50, 100, and 200 mg) of (a) YPO_4 (tetragonal phase) nanoparticles and (b) YPO_4:20% Ce (hexagonal phase) nanoparticles.

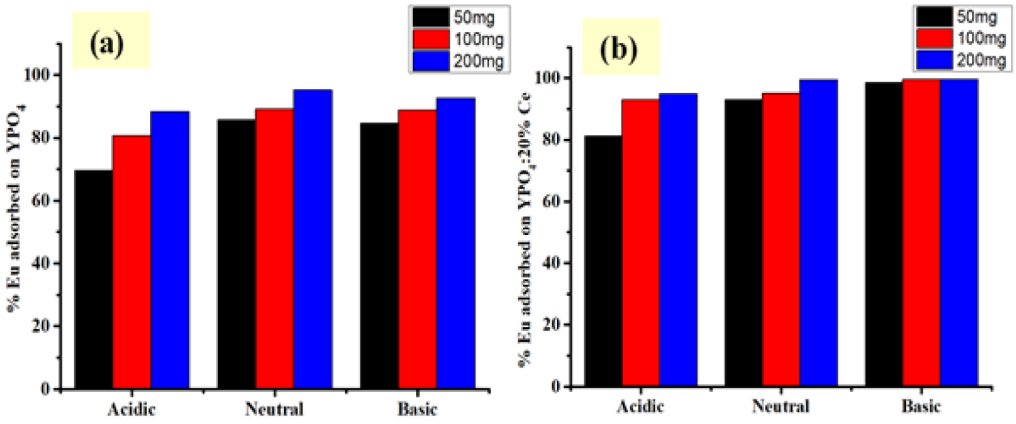

Figure 13. NAA data of supernatant separated after 60 ppm Eu^{3+} ions loaded on different amounts (X = 50, 100, and 200 mg) of (a) YPO_4 (tetragonal phase) nanoparticles and (b) YPO_4:20% Ce (hexagonal phase) nanoparticles.

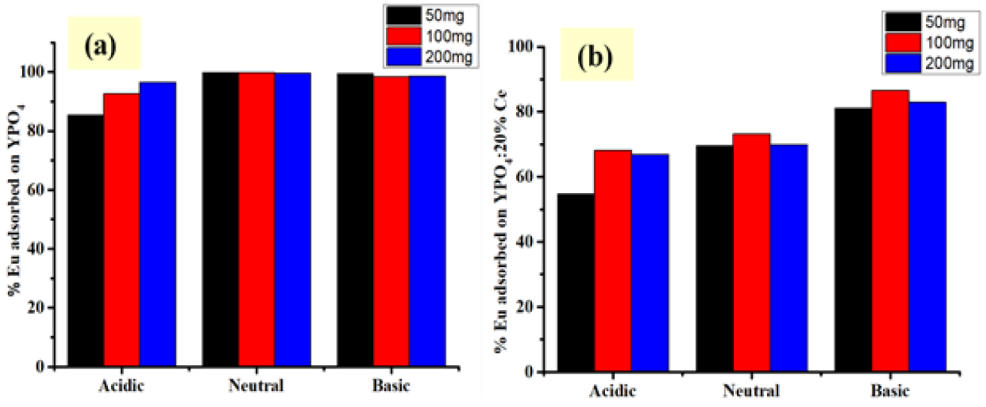

Figure 14. NAA data of supernatant separated after 40 ppm Eu^{3+} ions loaded on different amounts (X = 50, 100, and 200 mg) of (a) YPO_4 (tetragonal phase) nanoparticles and (b) YPO_4:20% Ce (hexagonal phase) nanoparticles.

luminescence intensity is very weak. However, the supernatant which was separated and tested using INAA reveals that there are ∼90−99% of Eu^{3+} ions left over in the tetragonal supernatant and ∼50−60% of Eu^{3+} ions left over in the hexagonal supernatant. So, in comparison with respect to the experiments of photoluminescence and INAA, the order of uptake of Eu^{3+} ions over nanoparticles is acidic < neutral < basic medium.

4. EXPERIMENTAL SECTION

4.1. Materials and Reagents. The reagents used were yttrium(III) acetate ($(CH_3CO_2)_3Y.xH_2O$, 99.99%), cerium-(III) acetate ($(CH_3CO_2)_3Ce.xH_2O$, 99.99%), ammonium dihydrogen phosphate ($NH_4H_2PO_4$, 99.99%), and europium-(III) acetate ($(CH_3CO_2)_3Eu.xH_2O$, 99.99%) were purchased from Sigma-Aldrich. In addition, there were dil. HCL and ethylene glycol (EG) for the synthesis of YPO_4 and YPO_4:20% Ce-doped nanoparticles.

https://doi.org/10.1021/acsomega.4c06813
ACS Omega 2025, 10, 14616−14625

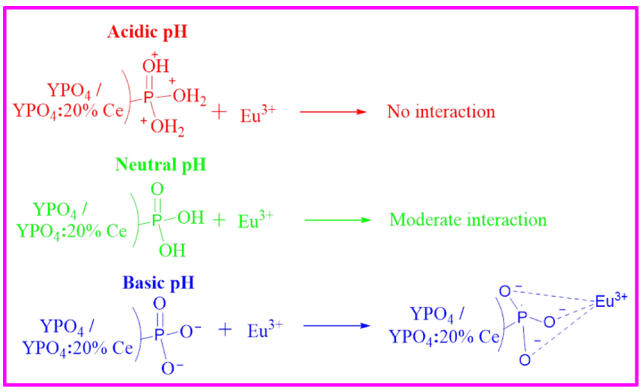

Figure 15. Schematic representation of a possible mechanism in the host−guest interaction.

4.2. Synthesis of YPO_4 and YPO_4:20% Ce Nanoparticles. Here, yttrium phosphate was synthesized in two different phases. Figure S2 shows a schematic diagram of the synthesis.

4.2.1. Tetragonal Phase (YPO_4). To begin with, 1 g of yttrium(III) acetate was weighed and transferred into a beaker. 5 mL of dil. HCL was added and heated until the acetate gets dissolved in acid. After its dissolution in acid, a minimum amount of deionized water was added for the evaporation of acid, and the process was repeated three to four times. Then, 0.5 g of ammonium dihydrogen phosphate was transferred into another beaker, which was further dissolved in distilled deionized water. After the acid evaporation, the yttrium(III) solution was transferred into a round-bottom (RB) flask for refluxing, and 30 mL of ethylene glycol (EG) was added as it not only acted as a capping agent but also helped in maintaining the reaction medium. After the temperature reached ∼75 °C, ammonium dihydrogen phosphate was added into the solution. Instantaneously, a white precipitate appeared in the RB. It was refluxed at 150 °C for about 2 h. After refluxing, it was cooled to room temperature and the mixture was centrifuged. The residue was collected and washed with 10 mL of acetone thrice and then dried under an IR lamp for 20 min to collect the nanoparticles in powder form.

The collected residue was examined by SEM and TEM for particle size determination and XRD for phase formation.

4.2.2. Hexagonal Phase (YPO_4:20% Ce). The synthesis of the hexagonal phase (YPO_4:20% Ce) is similar to the procedure described in Section 4.2.1. Here, 1 g of yttrium(III) acetate and 0.30 g of cerium(III) acetate were used as precursors.

4.3. Preparation of Eu-Acetate Solution (80, 60, and 40 ppm) in Distilled Water. For the preparation of 80 ppm Eu^{3+} ions, 43 mg of Eu (III) acetate was weighed and transferred into a beaker and evaporated under ∼80 °C by dissolving in conc. HCl and adding deionized water for the evaporation of acid. The above step was repeated twice or thrice. The collected solution was transferred into a 250 mL volumetric flask and deionized water was added to make it up to 250 mL of buffer solution/parent solution. Figure S3 shows a schematic diagram for the preparation of different Eu-acetate solutions. The same process was also repeated for the preparation of down to 60 and 40 ppm as the stock solution. This solution acts as a guest material in the following experiment.

4.4. Characterization Techniques. The phase and crystal structure of the YPO_4 nanoparticles were determined using a Rigaku, Miniflex-600 X-ray diffractometer (XRD) instrument with Ni-filtered Cu−K_α (1.5405 Å) radiation. The data was recorded at a scanning rate of 2° per minute in 2 theta of which the sample of YPO_4 was pasted on a glass slide by adding a small amount of methanol to achieve equal distribution and mounted on the sample holder.

The vibrational bands involved in the synthesized samples were studied by using Fourier transform infrared (FT-IR) spectroscopy via a Bomem MB 102 spectrophotometer with a 3 cm^{-1} resolution.

The surface morphology and qualitative elemental analysis of YPO_4 NPs were investigated under a scanning electron microscope (SEM) (Quanta FEG 450, FEI, the Netherlands), and the particle morphology was examined by using a transmission electron microscope (TEM) instrument (2000FX, JEOL, Japan).

In the case of photoluminescence investigation, down-shifting studies, i.e., excitation and emission spectra of all the samples, were recorded using an EDINBURGH Instrument FLS920 equipped with a 450 W xenon arc lamp.

The small samples (50 mg) were analyzed by IM-NAA for comparison purposes at the pneumatic carrier facility (PCF) of the Dhruva reactor (1 min neutron flux at 5 × 10^{13} n/cm^2/s), BARC.

■ ASSOCIATED CONTENT

Supporting Information

The Supporting Information is available free of charge at https://pubs.acs.org/doi/10.1021/acsomega.4c06813.

Typical XRD patterns and the stability of host materials at different pHs (Figure S1), schematic diagram of the synthesis procedure of YPO_4 (tetragonal phase) and YPO_4:20% Ce (hexagonal phase) nanoparticles (Figure S2), and schematic diagram of the experimental preparation of host−guest interaction studies of Eu (III) acetate solutions (80, 60, and 40 ppm) with YPO_4 and YPO_4:20% Ce-doped nanomaterials (at X = 50, 100, and 200 mg) (Figure S3) (PDF)

■ AUTHOR INFORMATION

Corresponding Authors

Venkata Nagendra Kumar Putta − *Department of Chemistry, GITAM University, Hyderabad 502329, India;* orcid.org/0000-0001-9029-2542; Email: pvenkatanagendrakumar@gmail.com

Raghumani Singh Ningthoujam − *Chemistry Division, Bhabha Atomic Research Centre, Mumbai 400085, India; Homi Bhabha National Institute, Mumbai 400094, India;* Email: rsn@barc.gov.in

Raghunath Acharya − *Isotope & Radiation Application Division, Bhabha Atomic Research Centre, Mumbai 400085, India; Homi Bhabha National Institute, Mumbai 400094, India;* Email: racharya@barc.gov.in

Authors

Ramaswamy Sandeep Perala − *Department of Chemistry, GITAM University, Hyderabad 502329, India; Chemistry Division, Bhabha Atomic Research Centre, Mumbai 400085, India; Isotope & Radiation Application Division, Bhabha*

https://doi.org/10.1021/acsomega.4c06813
ACS Omega 2025, 10, 14616−14625

Atomic Research Centre, Mumbai 400085, India; orcid.org/0000-0001-6042-5412

Bheeshma Pratap Singh − *Department of Physics, GITAM University, Visakhapatnam 530045, India;* orcid.org/0000-0001-9109-1515

Complete contact information is available at: https://pubs.acs.org/10.1021/acsomega.4c06813

Notes

The authors declare no competing financial interest.

■ ACKNOWLEDGMENTS

The authors thank the Operation crews of the Dhruva research reactor for their help in the INAA sample irradiation work. The authors from the GITAM University thank the Head, ChD, and the Head, RCD, BARC, for their support in this work. The authors from the GITAM University sincerely thank the Director, UGC-DAE-CSR Mumbai Centre for the Project on "Studies on lanthanides, actinides (U and Th) and toxic elements using nanoparticle based solid adsorbents and neutron activation analysis (NAA)". This is part of the PhD thesis work of Ramaswamy S. Perala, GITAM University, who is presently working at Gachon University, Republic of Korea.

■ REFERENCES

(1) Ningthoujam, R. S. *Enhancement of photoluminescence by rare earth ions doping in semiconductor inorganic*, Rai, S. B.; Dwivedi, Y. eds.; Nova Science Publishers Inc., USA, 2012pp. 145−182.

(2) Ghosh, P.; Oliva, J.; Rosa, E. D. L.; Haldar, K. K.; Solis, D.; Patra, A. Enhancement of Upconversion Emission of $LaPO_4$: Er@Yb Core-Shell Nanoparticles/Nanorods. *J. Phys. Chem. C* **2008**, *112*, 9650−9658.

(3) Parchur, A. K.; Ningthoujam, R. S. Preparation and Structure Refinement of Eu^{3+} Doped $CaMoO_4$ Nanoparticles. *Dalton Trans.* **2011**, *40*, 7590−7594.

(4) Rao, C. N. R.; Matte, H. S. S. R.; Voggu, R.; Govindaraj, A. Recent Progress in the Synthesis of Inorganic Nanoparticles. *Dalton Trans.* **2012**, *41* (17), 5089−5120.

(5) Wang, F.; Deng, R.; Wang, J.; Wang, Q.; Han, Y.; Zhu, H.; Chen, X.; Liu, X. Tuning Upconversion Through Energy Migration in Core-Shell Nanoparticles. *Nat. Mater.* **2011**, *10*, 968−973.

(6) Joshi, R.; Perala, R. S.; Shelar, S. B.; Ballal, A.; Singh, B. P.; Ningthoujam, R. S. Super Bright Red Upconversion in $NaErF_4$: 0.5% Tm@$NaYF_4$: 20%Yb Nanoparticles for Anti-counterfeit and Bioimaging Applications. *ACS Appl. Mater. Interfaces* **2021**, *13*, 3481−3490.

(7) Singh, B. P.; Perala, R. S.; Srivastava, M.; Ningthoujam, R. S. Synthesis of Nanostructured Materials by Thermolysis. In *Handbook on Synthesis Strategies for Advanced Materials*; Tyagi, A. K.; Ninghtoujam, R. S., eds.; Springer, Singapore, 2021, 333−382.

(8) Tang, Y.; Ouyang, M. Tailoring Properties and Functionalities of Metal Nanoparticles Through Crystallinity Engineering. *Nat. Mater.* **2007**, *6*, 754−759.

(9) Nie, Z.; Petukhova, A.; Kumacheva, E. Properties and Emerging Applications of Self-Assembled Structures made from Inorganic Nanoparticles. *Nat. Nanotechnol.* **2010**, *5*, 15−25.

(10) Singh, N. S.; Ningthoujam, R. S.; Devi, L. R.; Yaiphaba, N.; Sudarsan, V.; Singh, S. D.; Vatsa, R. K.; Tewari, R. Luminescence Study of Eu^{3+} Doped $GdVO_4$ Nanoparticles: Concentration, Particle Size, and Core/Shell Effects. *J. Appl. Phys.* **2008**, *104* (10), 104307.

(11) Singh, L. R.; Ningthoujam, R. S.; Sudarsan, V.; Srivastava, I.; Singh, S. D.; Dey, G. K.; Kulsheshtha, S. K. Luminescence study on Eu^{3+} doped Y_2O_3 nanoparticles: particle size, concentration and core−shell formation effects. *Nanotechnology* **2008**, *19* (5), 055201.

(12) Riwotzki, K.; Haase, M. Wet-Chemical Synthesis of Doped Colloidal Nanoparticles: YVO_4: Ln (Ln = Eu, Sm, Dy). *J. Phys. Chem. B* **1998**, *102*, 10129−10135.

(13) Xie, L.; Song, H.; Wang, Y.; Xu, W.; Bai, X.; Dong, B. Influence of Concentration Effect and Au Coating on Photoluminescence Properties of YVO_4: Eu^{3+} Nanoparticle Colloids. *J. Phys. Chem. C* **2010**, *114*, 9975−9980.

(14) Perala, R. S.; Joshi, R.; Singh, B. P.; Putta, V. N. K.; Acharya, R.; Ningthoujam, R. S. Brilliant Nonlinear Optical Response of Ho^{3+} and Yb^{3+} Activated YVO_4 Nanophosphor and Its Conjugation with Fe_3O_4 for Smart Anticounterfeit and Hyperthermia Applications. *ACS Omega* **2021**, *6*, 19471−19483.

(15) Perala, R. S.; Singh, B. P.; Putta, V. N. K.; Acharya, R.; Ningthoujam, R. S. Enrichment of Crystal Field Modification via Incorporation of Alkali K^+ Ions in YVO_4: Ho^{3+}/Yb^{3+} Nanophosphor and Its Hybrid with Superparamagnetic Iron Oxide Nanoparticles for Optical, Advanced Anticounterfeiting, Uranyl Detection, and Hyperthermia Applications. *ACS Omega* **2021**, *6*, 19517−19528.

(16) Perala, R. S.; Srivastava, M.; Singh, B. P.; Putta, V. N. K.; Acharya, R.; Ningthoujam, R. S. Altering of the Electric and Magnetic Dipole Transition Probability of Eu^{3+} in YPO_4 Lattice by Codoping of K^+ Ion: Potential Materials for Imaging and Heating. *Ind. Eng. Chem. Res.* **2022**, *61*, 9755−9762.

(17) Luwang, M. N.; Ningthoujam, R. S.; Jagannath; Srivastava, S. K.; Vatsa, R. K. Effects of Ce^{3+} Codoping and Annealing on Phase Transformation and Luminescence of Eu^{3+}-Doped YPO_4 Nanorods: D_2O Solvent Effect. *J. Am. Chem. Soc.* **2010**, *132*, 2759−2768.

(18) Luwang, M. N.; Ningthoujam, R. S.; Srivastava, S. K.; Vatsa, R. K. Disappearance and Recovery of Luminescence in Bi^{3+}, Eu^{3+} Codoped YPO_4 Nanoparticles Due to the Presence of Water Molecules Up to 800 °C. *J. Am. Chem. Soc.* **2011**, *133*, 2998−3004.

(19) Parchur, A. K.; Ningthoujam, R. S. Preparation, Microstructure and Crystal Structure Studies of Li^+ Co-doped YPO_4: Eu^{3+}. *RSC Adv.* **2012**, *2*, 10854−10858.

(20) Ivanets, A. I.; Srivastava, V.; Kitikova, N. V.; Shashkova, I. L.; Sillanpaa, M. Non-Apatite Ca-Mg Phosphate Sorbent for Removal of Toxic Metal Ions from Aqueous Solutions. *J. Environ. Chem. Eng.* **2017**, *5*, 2010−2017.

(21) Ivanets, A. I.; Srivastava, V.; Kitikova, N. V.; Shahkova, I. L.; Sillanpaa, M. Kinetic and Thermodynamic Studies of the Co(II) and Ni(II) Ions Removal from Aqueous Solutions by Ca-Mg Phosphates. *Chemosphere* **2017**, *171*, 348−354.

(22) Nenoff, T. M.; Miller, J. E.; Thoma, S. G.; Trudell, D. E. Highly Selective Inorganic Crystalline Ion Exchange Material for Sr^{2+} in Acidic Solutions. *Environ. Sci. Technol.* **1996**, *30*, 3630−3633.

(23) Kodama, T.; Harada, Y.; Ueda, M.; Shimizu, K.; Shuto, K.; Komarneni, S. Selective Exchange and Fixation of Strontium Ions with Ultrafine Na-4-mica. *Langmuir* **2001**, *17*, 4881−4886.

(24) Yang, D.; Sarina, S.; Zhu, H.; Liu, H.; Zheng, Z.; Xie, M.; Smith, S. V.; Komarneni, S. Capture of Radioactive Cesium and Iodide Ions from Water by Using Titanate Nanofibers and Nanotubes. *Angew. Chem., Int. Ed.* **2011**, *50*, 10594−10598.

(25) Bo, A.; Sarina, S.; Liu, H.; Zheng, Z.; Xiao, Q.; Gu, Y.; Ayoko, G. A.; Zhu, H. Efficient Removal of Cationic and Anionic Radioactive Pollutants from Water Using Hydrotalcite-Based Getters. *ACS Appl. Mater. Interfaces* **2016**, *8*, 16503−1510.

(26) White, D. A.; Labayru, R. Synthesis of a Manganese Dioxide-Silica Hydrous Composite and Its Properties as a Sorbtion Material for Strontium. *Ind. Eng. Chem. Res.* **1991**, *30*, 207−210.

(27) Duff, M. C.; Hunter, D. B.; Hobbs, D. T.; Fink, S. D.; Dai, Z.; Bradley, J. P. Mechanisms of Strontium and Uranium Removal from High-Level Radioactive Waste Simulant Solutions by the Sorbent Monosodium Titanate. *Environ. Sci. Technol.* **2004**, *38*, 5201−5207.

(28) Luca, V.; Tejada, J. J.; Vega, D.; Arrachart, G.; Rey, C. Zirconium(IV)-Benzene Phosphonate Coordination Polymers: Lanthanide and Actinide Extraction and Thermal Properties. *Inorg. Chem.* **2016**, *55*, 7928−7943.

(29) Singhal, P.; Jha, S. K.; Pandey, S. P.; Neogy, S. Rapid Extraction of Uranium from Sea Water Using Fe_3O_4 and Humic Acid Coated Fe_3O_4 Nanoparticles. *J. Hazard. Mater.* **2017**, *335*, 152−161.

(30) Singhal, P.; Jha, S. K.; Vats, B. G.; Ghosh, H. N. Electron-Transfer-Mediated Uranium Detection Using Quasi-Type II Core-

Shell Quantum Dots: Insights into Mechanistic Pathways. *Langmuir* **2017**, *33*, 8114−8122.
(31) Singhal, P.; Pulhani, V.; Ali, S. M.; Ningthoujam, R. S. Sorption of different metal ions on magnetic nanoparticles and their effect on nanoparticles settlement. *Environ. Nanotechnol. Monit. Manage.* **2019**, *11*, 100202.
(32) Polu, L.; Merah, S.; Jouini, N.; Fievet, F.; Villain, F. Synthesis of Inorganic Compounds (Metal, Oxide and Hydroxide) in Polyol Medium: A Versatile Route Related to the Sol-Gel Process. *J. Sol-Gel Sci. Techol.* **2003**, *26*, 261−265.
(33) Feldmann, C. Polyol-Mediated Synthesis of Nanoscale Functional Materials. *Adv. Funct. Mater.* **2003**, *13*, 101−107.
(34) Shannon, R. D. Revised Effective Ionic Radii and Systematic Studies of Interatomic Distances in Halides and Chalcogenides. *Acta Crystallogr.* **1976**, *A32*, 751.
(35) Singh, L. P.; Srivastava, S. K.; Mishra, R.; Ningthoujam, R. S. Multifunctional Hybrid Nanomaterials from Water Dispersible CaF_2: Eu^{3+}, Mn^{2+} and Fe_3O_4 for Luminescence and Hyperthermia Application. *J. Phys. Chem. C* **2014**, *118*, 18087−18096.
(36) Ningthoujam, R. S. Finding Confined Water in the Hexagonal Phase of $Bi_{0.05}Eu_{0.05}Y_{0.90}PO_4$: xH_2O and its Impact for Identifying the Location of Luminescence Quencher. *Pramana* **2013**, *80*, 1055−1064.
(37) Buhler, G.; Feldmann, C. Microwave-Assisted Synthesis of Luminescent $LaPO_4$: Ce, Tb Nanocrystals in Ionic Liquids. *Angew. Chem., Int. Ed.* **2006**, *45* (29), 4864−4867.
(38) Li, Q.; Yam, V. W.-W. Redox Luminescence Switch Based on Energy Transfer in $CePO_4$: Tb^{3+} Nanowires. *Angew. Chem., Int. Ed.* **2007**, *119*, 3556−3559.
(39) Kijkowska, R. Thermal Decompostion of Lanthanide Orthophosphates Synthesized through Crystallisation from Phosphoric Acid Solution. *Thermochim. Acta* **2003**, *404*, 81−88.
(40) Zollfrank, C.; Scheel, H.; Brungs, S.; Greil, P. E. (III) Orthophosphates: Synthesis, Characterization, and Optical Properties. *Cryst. Growth Des.* **2008**, *8*, 766−770.

https://doi.org/10.1021/acsomega.4c06813
ACS Omega 2025, 10, 14616−14625